Optica Applicata Vol. XI, No. 3, 1981

Correction of holographic concave gratings

REINER GÜTHER

Central Institute for Optics and Spectroscopy Academy of Sciences of the GDR, 1199 Berlin-Adlershof, Rudower Chaussee 5

The dimensioning of holographic gratings requires the following steps: selection of the grating type precalculation and automatic correction. The automatic correction should be based on a ray-tracing procedure in which we assume the gratings to be composed of infinitesimal plane gratings. We describe the diffraction of an incident ray by a local invariant vector formulation. As a merit function we use the Gauss moments of the spot diagrams. Examples of optimization are given for polychromators and monochromators including the related precalculations.

1. Introduction

The development of corrected holographic gratings requires the optimization of the latters. After selecting the grating type suitable for our problem, this optimization may be carried out in two steps: precalculation and automatic correction. The precalculation involves simple demands made upon the analytical formulae of aberration, which can be met at a low expense by using a small computer. Examples presented in [1] are given in Appendixes 1 and 2.

This precalculation is followed by an automatic optimization. A possible method is that of ray-tracing with the use of a merit function. This method was first applied to Seya-Namioka monochromators, as reported [2], where the ray tracing is carried out by varying the optical path. We use the diffraction by a local plane grating [7], which seems to be more convenient for systems containing gratings and for gratings produced by deformed spherical wavefronts. Some examples for polychromators and monochromators will be given.

2. Derivation of the formulae for ray-tracing

We use the notation as well as the coordinate system as given in [3], which are explained by fig. 1. C and D denote the point sources of laser light of the wavelength λ_0, which produces the interference pattern for preparing the grooves on the surface of the grating support. A is a point source emitting polychromatic light or a slit, and B is the image of A for the given wavelength λ. The distances of the points from the centre of the grating, S, are l_A, l_B, l_C, and l_D. The inplane angles (say α_I) and the offplane angles (say α_0) are defined

so that the three Cartesian coordinates of a point, say, the point A, are written in the form

$$(X_A, Y_A, Z_A) = (l_A \cos\alpha_I \cos\alpha_0,\ l_A \sin\alpha_I \sin\alpha_0,\ l_A \sin\alpha_0).$$

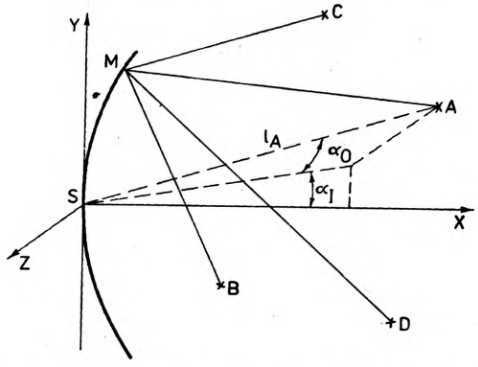

Fig. 1. Configuration for the preparation of holographic gratings by means of two light sources C and D, and for the reconstruction by using a point source A

The angles associated with B, C, and D are denoted by β, γ, and δ, respectively. While the grating is plotted, a local plane interference pattern appears at the point M (fig. 2) because infinitesimal plane waves arrive at M along

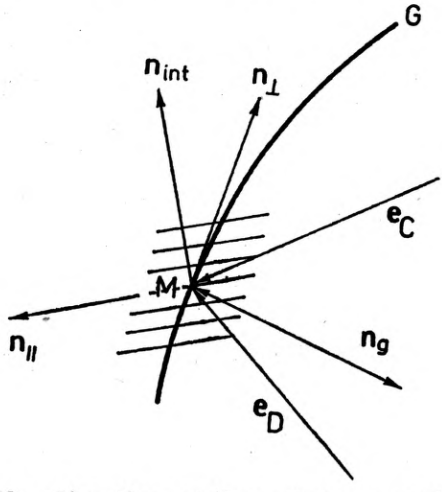

Fig. 2. Local Cartesian coordinate system generated by the local interference fringes

the direction unit vectors e_C and e_D, respectively, which point from C and D to M.

The spatial normal vector of the local system of interference fringes is given by $n_{\text{int}} = e_D - e_C$. The unit normal vector n_g at the point M on the support surface can be calculated in the usual manner. Now, the normalization of $n_g \times n_{\text{int}}$ yields the unit vector $n_\parallel$ parallel to the grooves of the grating (fig. 2). The unit vector $n_\perp$ perpendicular to the grooves can be constructed by normalizing $n_\parallel \times n_g$. The grating constant is given by

$$g = \lambda_0 / |n_{\text{int}} n_\perp|. \tag{1}$$

A ray emerging from the point A with a unit direction vector e_E pierces

the grating at the point M. The diffracted ray, characterized by the unit direction vector $\boldsymbol{e}_R$, can be then obtained, provided that (cf. [4], p. 450):

— the component of $\boldsymbol{e}_R$, parallel to $\boldsymbol{n}_\perp$ has to be calculated by using the grating equation,

— the component of $\boldsymbol{e}_R$, parallel to $\boldsymbol{n}_\parallel$ has to be calculated by using the law of reflection,

— the component of $\boldsymbol{e}_R$ parallel to $\boldsymbol{n}_g$ has to be calculated by using $||\boldsymbol{e}_R|| = 1$.

This means that

$$\boldsymbol{e}_R = r_g \boldsymbol{n}_g + r_\perp \boldsymbol{n}_\perp + r_\parallel \boldsymbol{n}_\parallel, \tag{2}$$

where

$$r_\perp = (\boldsymbol{e}_E \boldsymbol{n}_\perp) + k\lambda/g, \tag{3}$$

$$r_\parallel = (\boldsymbol{e}_E \boldsymbol{n}_\parallel), \tag{4}$$

$$r_g = -\operatorname{sgn}(\boldsymbol{e}_E \boldsymbol{n}_g)\sqrt{1 - r_\perp^2 - r_\parallel^2}\,. \tag{5}$$

In equation (5), the sgn-function yields the correct sign of the $\boldsymbol{n}_g$ component. In view of eqs. (1), (3), (4), and (5), eq. (2) is equivalent to the corresponding equation given in [5]. In contrast to the procedure given in [5], it seems that the use of the invariant vector formulation in the calculation of $\boldsymbol{e}_R$ is more convenient, especially if $\boldsymbol{e}_C$ and $\boldsymbol{e}_D$ are produced by deforming optical systems between the respective points C and D, and the grating, or if the grating is an element of a system.

For the support surface of the grating we assumed a toroidal surface shown in fig. 3, which is given by the relation

$$X = R_1 - \sqrt{\{\sqrt{R_2^2 - Z^2} + (R_1 - R_2)\}^2 - Y^2}. \tag{6}$$

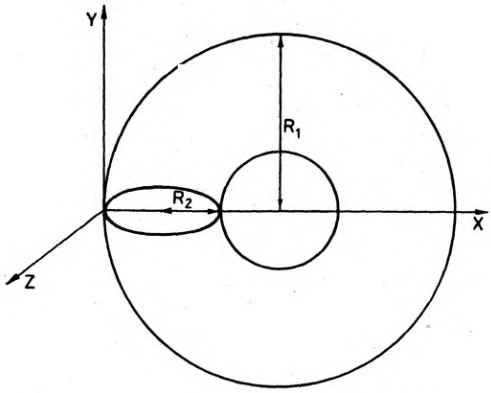

Fig. 3. Toroidal surface as a grating support

The piercing point M of the ray emerging from A on the surface (6) was calculated on the base of an approximation method using tangent planes, as described in [8].

The beam emerging from A was described in such a way that

$$e_E = -\begin{bmatrix}\cos(a_I + \Delta a_I)\cos(a_0 + \Delta a_0)\\ \sin(a_I + \Delta a_I)\cos(a_0 + \Delta a_0)\\ \sin(a_0 + \Delta a_0)\end{bmatrix}. \tag{7}$$

The angular deviations Δa_I and Δa_O from the straight line connecting A and S were varied within a range such that the required aperture ratio of the grating was ensured.

The rays of the pencil of light are intercepted by a plane (fig. 4).

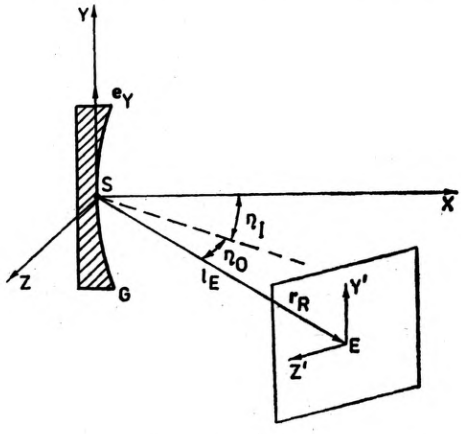

Fig. 4. Location of the interception plane

The principal ray is diffracted at the point S of the grating with the angles η_{inplane} and η_{offplane}. We choose the interception plane perpendicular to the diffracted principal ray extending at a distance l_E from S. There are several possibilities of the choice of $E \sim (l_E, \eta_I, \eta_O)$:

— For all wavelengths, E is identified with the meridional focal position. This means an optimization of the polychromator spectrum on the meridional focal curve.

— In the case of a monochromator, A and B are fixed in space, and the grating is moved to vary the wavelength. This movement can also be considered a suitably coupled movement of A and B, the grating being fixed. If the monochromator is based on a pure rotation of the grating, l_A and l_B remain constant for all the wavelengths and B is identified with E.

— l_E, η_I and η_O are varied for the purpose of optimization. Then the optimization is carried out in such a way that for all wavelengths the spot diagrams are minimized with respect to the merit criterion in one and the same interception plane. In this case we want to have a polychromator with a flat collecting surface for the spectrum.

The coordinate unit vectors of the local coordinate system in the interception plane are obtained by normalizing $(e_Y \times r_R)\, r_R$ and $e_Y \times r_R$. Here 1_R denotes the vector pointing in the direction of the diffracted principal ray. This vector extends from the grating to the interception plane. In the $Y' - Z'$

interception plane, the transverse aberration vector is equal to the difference between $\boldsymbol{r}_R$ and the point where the arbitrarily diffracted ray, indicated by the direction vector $\boldsymbol{e}_R$, pierces the interception plane. The projection of the transverse aberration vector upon the above mentioned normalized version of the direction vectors $(\boldsymbol{e}_Y \times \boldsymbol{r}_R)\boldsymbol{r}_R$ and $\boldsymbol{e}_R \times \boldsymbol{r}_R$ yields the two transverse aberration coordinates Y' and Z'.

The figure of merit employed is given by the Gauss moments of the transverse aberration coordinates. We looked for the minimum variance of the Y' and Z' coordinates of the points. The variance of the Y' coordinates was multiplied by a factor different from that of the Z' coordinates, because for an oblong slit the two dimensions of the spot image are interfering in a different manner. In our case the figure of merit does not include the Strehl's definition of brightness, since the resolution of the grating is far from the diffraction-theoretical value in the major part of the spectral ranges of the gratings.

3. Structure of the programme

The finally used figure of merit results from the addition of the Gauss moments of the spot diagrams for all equidistant wavelengths within a given interval for a light pencil emerging from the point A. In most cases the optimization was carried out for the central point of the slit. Every light pencil contained 9 to 49 rays. The number of wavelengths varied from 3 to 5.

The optimization was carried out by using a stochastic method. The parameters being free for variation were varied by random numbers. If by chance an improved merit function was obtained, the last configuration was stored by the computer. If no improvement resulted, the preceding configuration was taken as a basis to start a new trial. The merit function got stable after 400 to 600 steps. For these calculations a BESM 6 computer was used. Spot diagrams were plotted for the optimum configurations.

4. Results for a polychromator

The figure 5 shows the meridional and sagittal focal curves for a polychromator. The parameters for the preparation and use of the grating are: $\gamma_I = 45.264°$, $\delta_I = 0.917°$, $\alpha_O = \gamma_O = \delta_O = \eta_O = 0$, $l_C = 24.643$ cm, $l_D = 22.837$ cm, $\alpha_I = 44.805°$, $R_1 = R_2 = 20.17$ cm, $L_E = 18.80$ cm, and $\eta_I = 30.54°$. These parameters were calculated by using a variant of the precalculation procedure described in Appendix 1. In figure 5, the wavelength range from 800 nm to 822.9 nm is denoted by solid lines, while the dotted lines denote the characteristics of the grating up to 400 nm. There are two points of intersection (anastigmatic points) of the curves, one of which lies at 800 nm. Now, we optimize the grating by means of a single varying interception plane for all wavelengths.

The parameters being free for variation are α_I, l_A, $R_1 = R_2$, γ_I, l_C, l_D, η_I and l_E. The aperture ratio is 1 : 5, $\Delta = \gamma_I - \delta_I = 44.374^0$. If the programme works correctly, the anastigmatic point at 800 nm must be shifted from the boundary

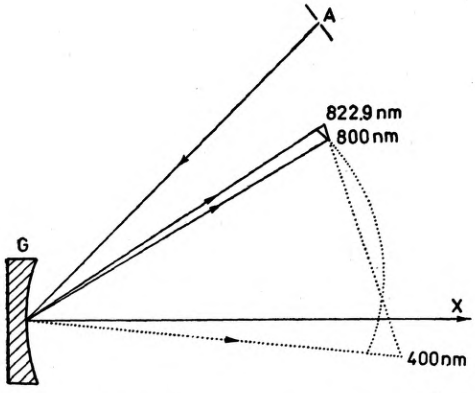

Fig. 5. Focal curves of a polychromator before the optimization

of the wavelength interval to its centre. Figure 6 shows that the result expected for the focal curves was obtained.

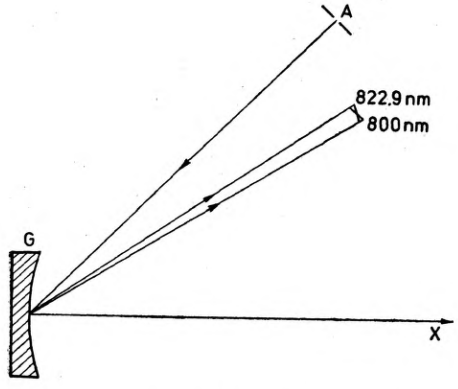

Fig. 6. Focal curves of a polychromator after the optimization

The parameters of the new configuration are $\eta_O = \gamma_O = \delta_O = \alpha_O = 0$, $\gamma_I = 44.213^0$, $\delta_I = -0.134^0$, $l_C = 23.586$ cm, $l_D = 21.88$ cm, $l_A = 22.279$ cm, $\alpha_I = 44.628^0$, $R_1 = R_2 = 20.477$ cm, $\eta_I = 30.635^0$, $l_E = 20.111$ cm. The spot diagrams shown in fig. 7 demonstrate the result. The top row contains the spot diagrams for three wavelengths at the beginning of the optimization.

The bottom row shows the variation of the spot diagrams after the optimization, where equal weights were attached to the height and the width of the spot diagrams. The concentration of the spots has been improved.

5. Results for monochromators

The case of a monochromator was tested with wavelength tuning by means of a pure rotation of the grating. The starting values for the monochromator precalculation programme, as described in Appendix 2, were $l_A = 40$ cm,

$l_B = 80$ cm, $R_1 = R_2 = R = 50$ cm, $\lambda_{max} = 600$ nm, $\lambda_m = 500$ nm, $\lambda_{min} = 400$ nm, $\Delta = \gamma_I - \delta_I = 30°$, $\varphi = \alpha - \beta = 20°$. Then the following configuration for an astigmatism = 0 and coma 1 = 0 resulted from the precalculation for $\lambda_m = 500$ nm, $R = 50$ cm, $l_C = 43.423$ cm, $l_D = 39.302$ cm, $\gamma_I = 26.883°$, $\delta_I = -3.111°$, $\gamma_O = \delta_O = \alpha_O = 0$, $\alpha_I(500\text{ nm}) = 26.305°$. This is the starting configuration for the automatic correction. The top row of fig. 8 shows the

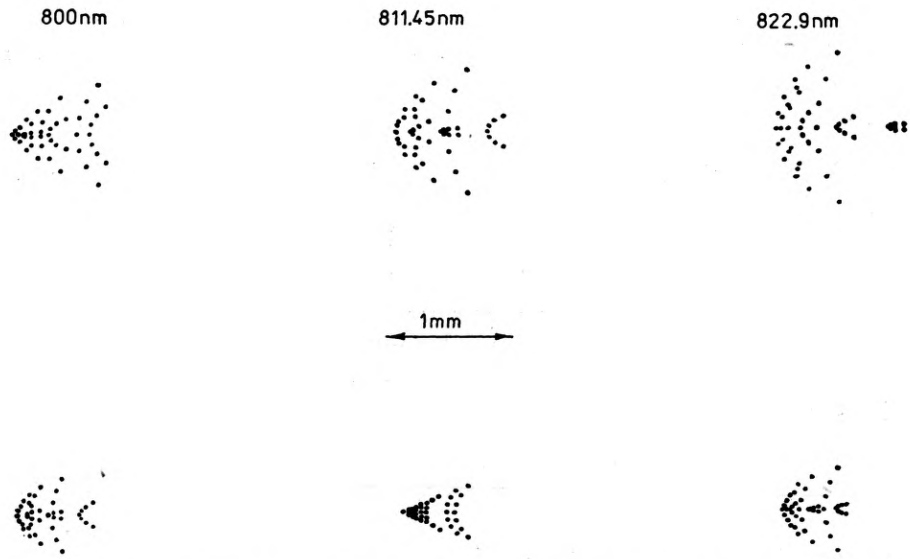

Fig. 7. Spot diagram for a polychromator before and after the optimization

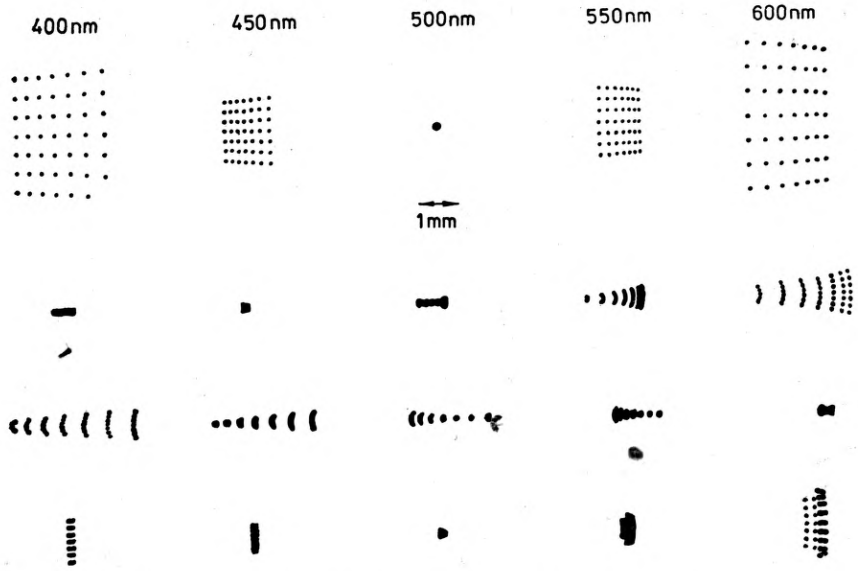

Fig. 8. Spot diagram for a monochromator before and after the optimization

spot diagrams for this starting configuration for five wavelengths. The second row shows the spot diagrams plotted after the automatic optimization, where equal weights were attached to the height and the width of the spot diagrams. In this case the programme favours the height reduction. The third row is obtained by emphasizing reduction of height. If the width reduction is emphasized, as is preferable for monochromators, then the lowermost row results. The configuration of the grating for the last-mentioned monochromator is given by $R = 52.803$ cm, $l_C = 42.179$ cm, $l_D = 41.488$ cm, $\gamma = 26.588°$, $\delta_I = -3.412°$, $\alpha_I(500\ \text{nm}) = 26.324°$, $\alpha_O = \gamma_O = \delta_O = 0$. The efficiency of the optimization is obvious.

6. Conclusion

The principal work has to be done in the precalculation, because the type of grating is given by this computational step. In most cases the automatic correction cannot test all of the possible cases. Thus, only a local optimum is looked for. Generally, we do not look for an "unexpected new type" of the grating to be obtained by automatic correction, but only for a maximum utilization of all the possibilities offered by the chosen type of grating.

Appendix 1

A possible precalculation for polychromators

Precalculations can be done by using analytical formulae for the different types of aberration as described in the literature e.g. in [3] or [6]. For selected wavelengths, these aberrations can be subject to several restrictions, for example, they can be required to be zero. Then we obtain sets of equations for the free parameters. Frequently, the number of the actually free parameters is limited by the respective application.

The figure A1 shows a pair of general focal curves of a corrected concave grating. The po-

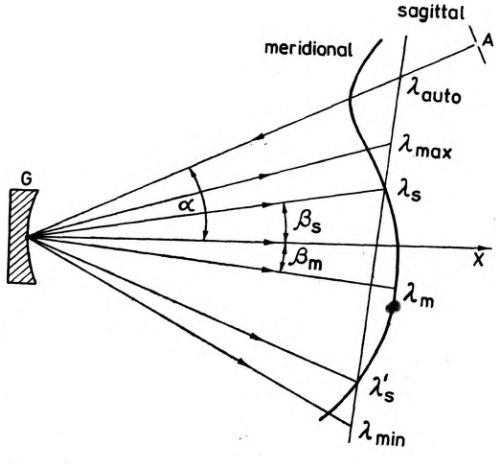

Fig. A1. Meridional focal curve M, sagittal focal curve S, slit A and grating G in a polychromator configuration

sition of the slit A is required to be given by the wavelength of autocollimation, λ_{auto}, which means a back-diffraction into the direction of incidence. Let the two curves intersect at λ_s. At λ_s the tangents of both focal curves shall be parallel to each other. These conditions determine the range of "symmetrical" correction. For the sake of mathematical simplicity we assume $l_C = l_D$. The input $\gamma - \delta$ fixes the approximate number of grooves per mm of the grating, the approximate value g of the grating constant being $\lambda_0/2 \sin(\gamma - \delta)/2$. The complete set of inputs comprises λ_0, λ_{auto}, λ_s, λ_m, R, l_C, and $\gamma - \delta$. The obtained set of equations can be transformed into a single equation for one unknown, $v = (\gamma + \delta)/2$, by successive elimination:

$$\alpha = \arcsin(k\lambda_{\text{auto}} \cos v/2g), \tag{A1}$$

(grating equations for λ_{auto});

$$\beta_s = \arcsin(k\lambda_s \cos v/g - \sin\alpha), \tag{A2}$$

(grating equation for λ_s);

$$\beta_m = \arcsin(k\lambda_m \cos v/g - \sin\alpha), \tag{A3}$$

(grating equation for λ_m);

$$(R/B) = (1 - 2(R/l_C)\cos v\sqrt{1 - (\lambda_0/2g)^2}\tan v, \tag{A4}$$

(notation B);

$$(R/l_A) = \cos^2\beta_s[\{\cos\alpha + \cos\beta_s + (\sin\alpha + \sin\beta_s)(R/B)\} / \cos^2\beta_s - \cos\alpha - \cos\beta_s - (\sin\alpha + \sin\beta_s)\tan v]/(\cos^2\alpha - \cos^2\beta_s), \tag{A5}$$

(astigmatism at λ_s);

$$(A/R) = -(R/l_A)\cos^2\alpha + \cos\alpha + (R/B)\sin\alpha, \tag{A6}$$

(notation A);

$$S = 2\tan\beta_m + (\sin\beta_m - (R/B)\cos\beta_m)/((AR) + \cos\beta_m + (R/B)\sin\beta_m), \tag{A7}$$

(notation S);

$$(S\tan\beta_m + 1)/(S - \tan\beta_m) = (1 - (R/l_A)\cos\beta_m + \cos\alpha\cos\beta_m + \cos\beta_m\sin\alpha\tan v) / (\tan v - (R/l_A)\sin\beta_m + \sin\beta_m\cos\alpha + \sin\beta_m\cos\alpha\tan v), \tag{A8}$$

(parallel tangents at λ_m).

All of the angles are inplane angles, λ_0 is the wavelength used in the preparation of the grating. After a successive substitution of (A1) through (A7), eq. (A8) can be solved for v by means of Newton's algorithm using a small computer. From the resulting v and the given quantity $\gamma - \delta$ one obtains γ and δ, and from these values the whole configuration is derived. Optimal courses of the focal curves are obtained by a suitable choice of λ_{auto}, λ_s, and λ_m.

Appendix 2

A possible precalculation for monochromators

The figure A2 shows a monochromator tuned by a rotation of the grating. The following parameters are given: l_A, l_B, No. of grooves/mm, subject to the condition $\Delta = \gamma - \delta$ (see Appendix 1), the wavelength λ_s at which the astigmatism as well as coma 1 are zero, the radius of curvature, R, of the support, and the angle φ between A, S, and B. From these

conditions, a set of equations for one unknown γ can be derived:

$$H = k\lambda_s(\sin\gamma - \sin\delta)/\lambda_0, \tag{A9}$$

$$\alpha = \arcsin(H/2 - \sqrt{H^2/4 - (H^2 - \sin^2\varphi)/(2(1+\cos\varphi))}), \tag{A10}$$

(grating equation for λ_s);

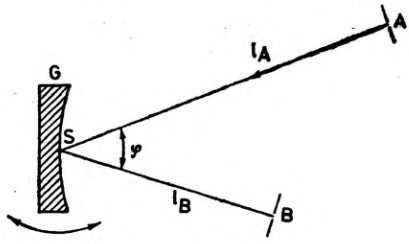

Fig. A2. Fixed slit A, fixed slit image B, and rotated grating G in a monochromator configuration

$$\beta = \alpha - \varphi, \tag{A11}$$

$$B = \lambda_0(1/l_B - (\cos\beta_s + \cos\alpha_s)/R + 1/l_A)/(k\lambda_s) + (\cos\gamma - \cos(\gamma - \Delta))/R, \tag{A12}$$

(notation B);

$$K_1 = B\sin\delta\cos^2\delta - (\sin\gamma\cos\gamma - \sin\delta\cos\delta)/(2R), \tag{A13}$$

$$K_2 = \sin\gamma\cos^2\gamma - \sin\delta\cos^2\delta, \tag{A14}$$

$$K_3 = -(B^2\sin\delta\cos^2\delta/2 - B\sin\delta\cos\delta/(2R)) - \lambda_0 K_4/(k\lambda_s), \tag{A15}$$

$$K_4 = (\cos\alpha/l_A - 1/R)\sin\alpha\cos\alpha/(2l_A) + (\cos\beta/l_B - 1/R)\sin\beta\cos\beta/(2l_B) \tag{A16}$$

notations K_1 through K_4);

$$1/l_C = -K_1/K_2 + \sqrt{(K_1/K_2)^2 - 2K_3/K_2}, \tag{A17}$$

(astigmatism at λ_s);

$$1/l_D = 1/l_C - B, \tag{A18}$$

$$0 = -\cos^2\beta/l_B - \cos^2\alpha/1_A + (\cos\alpha + \cos\beta)/R + k\lambda_s(\cos^2\gamma/l_C - \cos\gamma/R - \cos^2\delta/l_D + \cos\delta/R)/\lambda_0 \text{(coma 1 = 0 at } \lambda_s). \tag{A19}$$

Using (A9) through (A19), from (A19) one obtains the solution γ by means of Newton's algorithm. The configuration of the grating can be derived from γ.

Acknowledgement – The author is indebted to S. Polze for helpful discussions, and to H. Heimberg for computational assistance.

References

[1] GÜTHER R., HEIMBERG H., POLZE S., 11. *Frühjahrsschule Optik, Masserberg/Thür.*, 26.–28, 3, 1979, Physikalische Gesellschaft der DDR.

[2] TAKAHASHI A., KATAYAMA T., J. Opt. Soc. Am. **68** (1978), 1254.

[3] HAYAT G. S., FLAMAND J., LACROIX M., GRILLO A., Optical Engineering **14** (1975), 420.

[4] Stroke G. W., Diffraction Gratings, [in] *Handbuch der Physik*, ed. S. Fülge, Vol. 24 Springer-Verlag, Berlin, Heidelberg, New York 1967, p. 450.
[5] Noda H., Namioka T., Seya M., J. Opt. Soc. Am. **64** (1974), 1037.
[6] Noda H,, Namioka T., Seya M., J. Opt. Soc. Am. **64** (1974), 1031.
[7] Güther R., 12. *Frühjahrsschule Optik, Dresden*, 31.3.–2.4. 1980, Physikalische Gesellschaft der DDR, pp. 20.
[8] Welford W. T., *Aberration of the Symmetrical Optical System*, Academic Press, London, 1974, p. 57.

Received November 24, 1980

Коррекция голографиеских вогнутых сеток

Определение размеров голографических сеток требует принятия следующих мер: выбора типа сетки, предварительного пересчёта, а также автоматической коррекции. Автоматическая коррекция должна быть основана на пересчётах пучка лучей. В нашем методе пересчёта принято, что сетки состоят из бесконечных плоских сеток. Описана дифракция луча, падающего с помощью локально инвариантных векторов. В качестве функций цели были использованы моменты Гаусса для следовой диаграммы (spot diagram). Примеры оптимизации приведены для полихроматоров, а также монохроматов вместе с предварительными расчётами.